

# **RAPID DROPS OF OCEAN TEMPERATURES IN SEVERAL SHALLOW BAYS IN NOVA SCOTIA DURING A RECENT COLD AIR OUTBREAK**

MICHAEL P. CASEY<sup>1\*</sup>, BRIAN PETRIE<sup>2</sup>,  
YOUYU LU<sup>1</sup>, SARAH MACDERMID<sup>1,3</sup>  
AND JEAN-PHILIPPE PAQUIN<sup>3</sup>

*<sup>1</sup>Fisheries & Oceans Canada,  
Bedford Institute of Oceanography,  
Dartmouth, NS*

*<sup>2</sup>Halifax, NS*

*<sup>3</sup>Division de la Recherche en Météorologie,  
Environnement et Changement Climatique Canada,  
Dorval, QC*

## **ABSTRACT**

From February 3-5, 2023 Atlantic Canada experienced an extreme cold Arctic air outbreak with high winds that set many local meteorological records, including wind chills as low as  $-47^{\circ}\text{C}$ . The impacts of the cold air outbreak on ocean temperatures and ice formation are investigated using predictions from the Coastal Ice-Ocean Prediction System for the East Coast of Canada (CIOPS-E), developed by Environment and Climate Change Canada. Observations from moorings further inform the predictions. The analysis suggests that during the event, several shallow bays and coastal areas in Nova Scotia experienced significant, abrupt temperature decreases ranging from  $1.0$  to  $3.9^{\circ}\text{C}$ . Overall cooling estimated by the model was  $2.3^{\circ}\text{C}$  for nearshore locations where observations recorded an average temperature decrease of  $3.0^{\circ}\text{C}$ . On the other hand, at individual sites the difference between observed and modelled cooling was up to  $2.4^{\circ}\text{C}$ . This difference can be attributed partly to the fact that the model does not adequately resolve the coastline features of some of the nearshore mooring sites.

In comparison, we also analyze another cold air outbreak that occurred on December 15-18, 2016, with wind chills as low as  $-37^{\circ}\text{C}$ . The ocean temperatures changes associated with this earlier event saw decreases of  $0.8$  to  $3.5^{\circ}\text{C}$ , potentially contributing to an ongoing fish kill in St. Mary's Bay (near the mouth of the Bay of Fundy) at the time.

\* Author to whom correspondence should be addressed:  
michael.casey@dfo-mpo.gc.ca

Keywords: Ocean temperature, Cold air outbreak, Ocean forecasting, Shallow bays, Nova Scotia

## INTRODUCTION

Cold air outbreaks (CAOs) are large-scale, low temperature atmospheric intrusions. While they often last for more than five days, a fast-moving CAO can be a short-lived event that can significantly impact a region. Atlantic Canada wintertime CAOs are usually caused by intrusions of cold Arctic air; their frequency and duration have decreased in the late 2010s compared to the late 1970s (Smith & Sheridan 2020).

On Feb. 3-5, 2023, Atlantic Canada experienced a fast-moving, short-lived CAO. Low temperatures combined with high winds brought extreme wind chill values at many locations. For example, at Halifax Stanfield International Airport the wind chill reached  $-43^{\circ}\text{C}$ , while at Saint John, New Brunswick it was  $-47^{\circ}\text{C}$ . Such extreme weather conditions can cause significant changes in ocean conditions such as a drop in ocean temperatures that could be stressful to marine life. Fish-kill events have been observed during CAOs on Okinawa-jima Island, Japan in 2023 (Gomez *et al.* 2024) and in Florida in January 1977 (Gilmore *et al.* 1978). Sudden intrusions of cold water have also resulted in a massive tilefish kill off the mid-Atlantic Bight immediately southwest of the Gulf of Maine (Marsh *et al.* 1999). In a news release, February 2022, Seaward Enterprises Association of Newfoundland and Labrador Inc. has attributed a large mackerel kill in December 2021 off the east coast of Newfoundland to cold water (fisherynation.com). St. John's weather records indicate a sustained period of average air temperature of  $-2.8^{\circ}\text{C}$  (minimum  $-11.4^{\circ}\text{C}$ ) accompanied by average winds of 30 km/h (maximum 71 km/h) which could have been the cause of the ocean cooling; the average (minimum) wind chill was  $-11.4^{\circ}\text{C}$  ( $-18^{\circ}\text{C}$ ) from Dec. 14 to 31. In Nova Scotia, another CAO in mid-December 2016 may have contributed to a significant fish kill event in St. Mary's Bay, however the evidence is inconclusive (Foley *et al.* 2019, Department of Fisheries and Oceans Canada 2017). (Note that wind chill, which depends on air temperature and wind speed, is an indicator of the potential for heat loss, and is used here as a reference for which people are generally familiar. The models used in this study explicitly estimate all

heat exchanges between the atmosphere and ocean as outlined in the references below.)

Given the potential impacts of rapid ocean cooling during intense CAOs, identifying the most threatened areas to such extreme events may be used to industry advantage, such as for aquaculture site selection. With operational ocean and weather predictions available, forecasting extreme events several days in advance could help industry to develop mitigation measures.

Here, we investigate the impacts of the February 2023 and December 2016 CAOs on ocean temperatures using both *in-situ* observations from moored instruments, and results from the high-resolution Coastal Ice Ocean Prediction System for the East Coast of Canada (CIOPS-E) ocean model (Paquin *et al.* 2021, 2022, 2024; see Fig 1 for model domain and bathymetry) obtained from Environment and Climate Change Canada (ECCC). Wind and air temperature observations from ECCC are used to quantify the timing and intensity of the CAOs over the region. The locations and magnitudes of significant water temperature changes are determined and their causes are discussed.

## OCEAN MODEL AND OBSERVATIONS

We use both *in-situ* observations and model results to investigate the ocean temperature response to the CAOs. The observations are mainly from wharf-mounted instruments for the February 2023 event, and from both moorings and sensors deployed in lobster pots during the December 2016 CAO. The model and observations are complementary: the model provides broad scale coverage of ocean variables including ice; the coastal observation sites provide data for areas where the model does not resolve the topography well and have the potential to suggest improvements to the model.

### CIOPS-E model

CIOPS-E has been run operationally at ECCC since 2021 (Paquin *et al.* 2021, 2022, 2024). The CIOPS-E system uses the Nucleus for European Modeling of the Ocean version 3.6 (NEMO, Madec *et al.* 2015) coupled to Los Alamos Community Ice Code (CICE, Hunke 2001, Lipscomb *et al.* 2007, Hunke and Lipscomb 2008) to produce simulations of the ocean and sea ice conditions over the East Coast of Canada and the Gulf of St. Lawrence. Briefly, CIOPS-E delivers two main products: 1) a continuous simulation using spectral

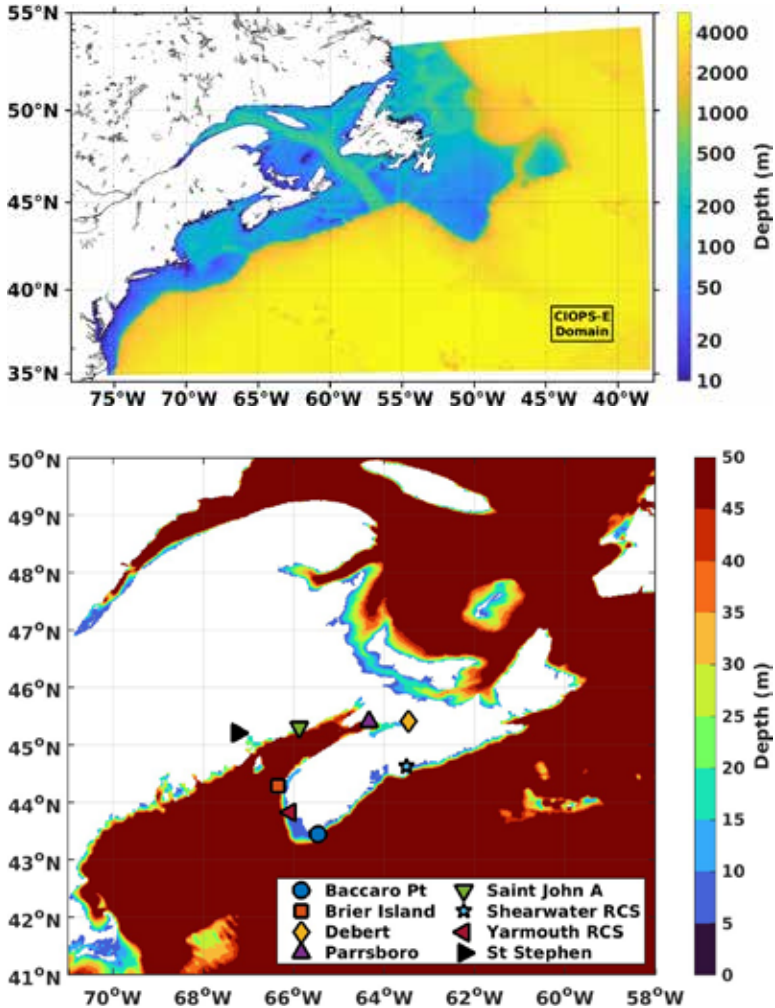


Fig 1 CIOPS-E full-domain bathymetry (m, top) and zoomed-in area of interest (m, bottom), using different color scales to emphasize the shallow areas and bays. The bottom panel also shows ECCC weather stations adjacent to the coastal areas of Nova Scotia and New Brunswick used in this study.

nudging, referred to as a “pseudo-analysis”; and 2) a short-term 48-hour forecast produced four times daily. The CIOPS-E horizontal resolution is approximately 2 km at the latitude of Nova Scotia. In the vertical, CIOPS-E concentrates 20 of its total 100 vertical levels in the first 30 m of the water column to better represent near-surface

ocean processes and heat exchanges. The minimum water depth is 7.5 m in the area around Nova Scotia and in the Bay of Fundy.

CIOPS-E solves the governing equations for ocean currents, sea level, temperature and salinity, and the formation, melting, movement and deformation of sea ice. The atmospheric forcing used to provide surface conditions to the ocean model comes from a combination of two Numerical Weather Predictions models, also running operationally at ECCC. Short-term forecasts from the High-Resolution Deterministic Prediction System (HRDPS, Mildbrandt *et al.* 2016) and the Global Deterministic Prediction System (GDPS, Gasset *et al.* 2019) are combined to provide continuous and coherent hourly forcing for the ocean model. The atmospheric forcing variables include near-surface wind, temperature and humidity, incoming radiative fluxes (solar and infrared), and freshwater fluxes from precipitation and climatological river runoffs. The main tidal constituents are imposed at the model lateral boundaries (elevation and transport), and propagation of the tides in the model domain interior is resolved explicitly. The non-tidal conditions for temperature, salinity, and ocean currents are also provided at the model open boundaries from ECCC's Regional Ice-Ocean Prediction System (RIOPS, Smith *et al.* 2021). To assure the consistency of the large-scale circulation in the pseudo-analysis, a spectral nudging method is used to correct CIOPS-E's three-dimensional temperature and salinity fields towards RIOPS' data-assimilative solution (i.e. constrained by *in-situ* and satellite observations). The spectral nudging method in CIOPS-E is applied only off the continental shelf to constrain the large-scale features, such as the Gulf Stream eddies and meanders. In our area of interest on the shelf, the CIOPS-E solution is not constrained, allowing the model to fully take advantage of CIOPS-E's high resolution. Detailed discussions on the model implementation can be found in Paquin *et al.* (2024). The pseudo-analysis simulation covers the period from November 2015 to present, therefore allowing comparison with observations for both CAOs (2016 & 2023).

### Observations

*In-situ* temperature data, sampled hourly, were collected by moored instruments deployed in lobster traps on the ocean floor by the Fishermen and Scientists Research Society (FSRS, fsrsns.ca; December 2016 CAO only), and by instruments deployed and maintained at

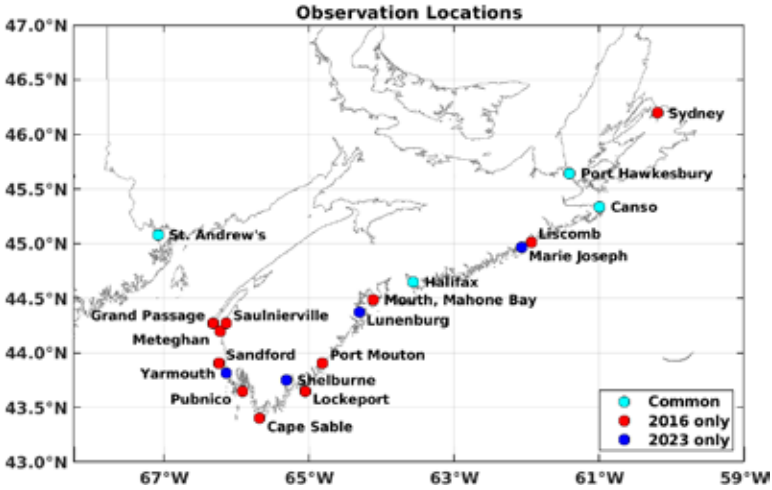


Fig 2 Ocean temperature observation sites for the 2016 (red) and 2023 (blue) CAOs, and the sites common to both events (cyan).

wharfs by the Bedford Institute of Oceanography (BIO), Department of Fisheries and Oceans (DFO) Canada, and St. Andrews Biological Station (StA), DFO (both CAOs), see Fig 2 for locations. Table 1 provides detailed information for each mooring (location, depth of deployment, type of deployment, and data collection agency). Sensors deployed in lobster pots measured sea-bottom temperature at that location, other sensors took measurements at the indicated depths.

For each instrument site, nearby model points were chosen for comparison. However, the detailed coastline at some sensor locations is not resolved by the model. In those cases, the nearest model point was chosen for comparison. This led to differences in depth (Model – Instrument) of  $\sim +80$  m to  $-16$  m (Table 1). The names of the FSRS sites are taken from the nearest geographical location of note and do not necessarily indicate that the instrument was deployed at the exact location from which the name is taken, e.g., Lockeport.

## FEBRUARY 2023 COLD AIR OUTBREAK

### Meteorological conditions

For the CAO of Feb. 3-5, 2023, Fig 3 presents a map of predicted 1.5 m air temperatures and 10 m winds speeds from the HRDPS of the Canadian Meteorological Centre (Milbrandt *et al.* 2016) at the

**Table 1** Mooring site locations and characteristics for observations for the 2016 and 2023 CAOs. Also indicated are site bottom depths and temperature changes from model results and observations. Observation data sources are: St. Andrew's Biological Station (StA), DFO; Fishermen and Scientists Research Society (FSRS); Bedford Institute of Oceanography (BIO), DFO. StA and BIO sites were located at wharfs at the indicated depths, FSRS sites were deployed in lobster traps on the ocean floor.

2016 Sites	Instrument	Bottom Depth (m)		$\Delta T$ ( $^{\circ}\text{C}$ )		Source
	Depth (m)	Obs.	Model	Obs.	Model	
St. Andrew's	2	< 10	24.6	1.7	1.3	StA
Grand Passage	7	7	12.8	1.4	2.0	FSRS
Saulnierville	17	17	10.8	1.2	2.5	FSRS
Meteghan	29	29	12.8	1.0	1.7	FSRS
Sandford	33	33	21.0	1.6	0.4	FSRS
Pubnico	18	18	7.3	2.5	2.5	FSRS
Cape Sable	26	26	8.9	1.8	6.3	FSRS
Lockeport	14	14	24.6	1.0	2.3	FSRS
Port Mouton	3	3	7.3	1.1	2.4	FSRS
Mouth, Mahone Bay	7	7	7.3	1.9	3.9	FSRS
Halifax	2	< 10	8.9	1.2	1.1	BIO
Liscomb	13	13	10.8	2.4	2.1	BIO
Canso	3	< 10	82.2	3.7	1.5	BIO
Port Hawkesbury A	1.5	< 10	10.8	3.1	1.2	BIO
Sydney	1.5	< 10	8.9	2.4	2.2	BIO
2023 Sites						
St. Andrew's	1	< 10	24.6	2.1	2.1	StA
Yarmouth	2	< 10	8.9	3.9	2.2	BIO
Shelburne	1	< 10	7.3	2.9	3.5	BIO
Lunenburg	5	< 10	7.3	3.8	3.2	BIO
Halifax	2	< 10	8.9	1.0	2.2	BIO
Marie Joseph	2	< 10	10.8	3.0	2.8	BIO
Canso	3	< 10	82.2	3.7	1.3	BIO
Port Hawkesbury B	3	< 10	10.8	3.5	1.1	BIO

peak of the event on Feb. 4, 12:00 AST (Atlantic Standard Time; unless noted, all times are in AST). The map illustrates the large geographical extent of the CAO, the coherence of the wind forcing, and air temperatures of about  $-16^{\circ}\text{C}$  to  $-20^{\circ}\text{C}$  in the area of interest.

Surface air temperature and wind-chill time series (top panel, Fig 4) from selected ECCC weather stations around the Bay of Fundy and Nova Scotia (bottom panel, Fig 1) give a timeline of events (ECCC 2023). The cold air reached stations in southern New Brunswick and Nova Scotia a few hours after Feb. 3, 00:00, with air temperatures returning to pre-outbreak values by the latter half of Feb. 5. The coldest temperatures were recorded in southern New Brunswick, the warmest in southwest Nova Scotia (SWNS). Although



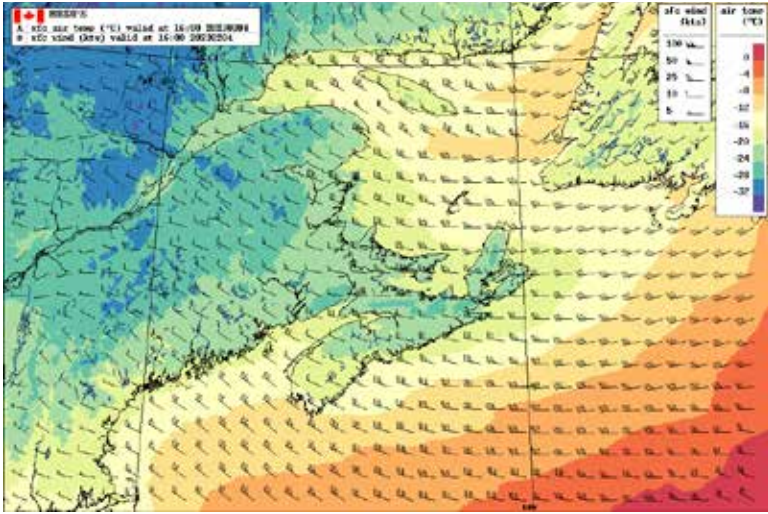


**Fig 3** HRDPS-predicted 1.5 m air temperatures ( $^{\circ}\text{C}$ ) and 10 m winds (kts, 1 kt = 1.852 km/h) on Feb. 4, 2023, 12:00 AST (16:00 UTC).

hard to precisely define, as the timing is slightly different at each site, the grey-shaded areas in Fig 4 (and subsequent Figs) delimit the approximate temporal extent of the CAO based on air temperatures. The event begins at St. Stephen and propagates to the south-east, with Shearwater the last site affected. An analysis of correlations between the two sites shows Shearwater lagging St. Stephen by 4 h. Over this period, the average correlation among the air temperature series was 0.95 with a standard deviation of 0.04. During the event, the average temperature at the warmest site, Baccaro Point, was  $8.8^{\circ}\text{C}$  greater than that at St. Stephen and Saint John, the coldest sites. Air temperatures dropped from the range of  $+5$  to  $-5^{\circ}\text{C}$  to between  $-18$  and  $-27^{\circ}\text{C}$  in less than a day, and then returned to pre-outbreak temperatures by 1.5 days after the minimum.

Throughout the CAO, winds were predominately west-north-westerly (WNW), with pre-outbreak speeds of 5 to 20 km/h, which increased to peak values of 20 to 70 km/h around Feb. 4, 00:00 (middle and bottom panels, Fig 4). Winds then slackened to 0 to 10 km/h at around Feb. 5, 00:00. Some locations, such as the Yarmouth Reference Climate Station (RCS) then saw a slight re-intensification of wind speeds to 10 to 40 km/h, with a directional change to southwesterly for the last few hours of the CAO. The combined cold



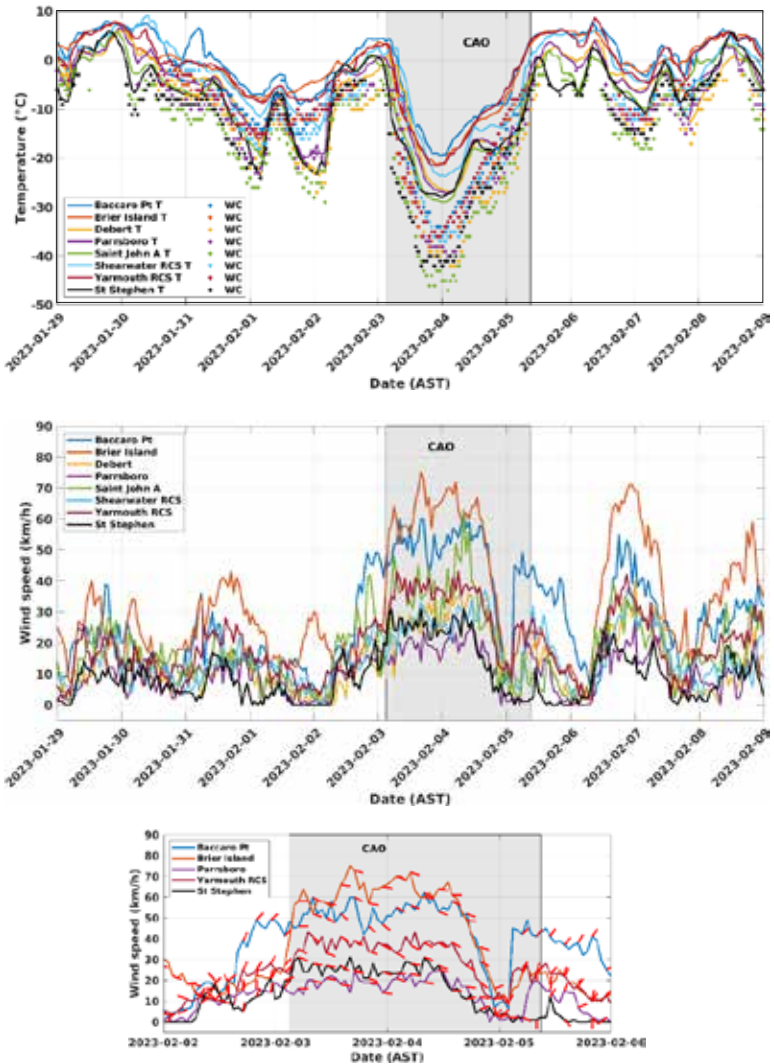


**Fig 4** Top panel: air temperatures ( $^{\circ}\text{C}$ ; solid lines) and wind chills (WC; $^{\circ}\text{C}$ ; '+' symbol) as measured by the ECCO stations in Fig 1. Middle panel: wind speeds (km/h) at the same sites. Bottom panel: wind speed (solid lines) and 'to' directions (short red lines) for a shorter period around the CAO for select representative sites. Winds were generally to the east-southeast during February 3-5, 2023.

air temperatures and wind speeds resulted in extreme wind chills ranging between  $-34$  to  $-45^{\circ}\text{C}$  on Feb. 4, 00:00 (top panel, Fig 4). The variation of wind chill during the CAO was very similar to the

air temperature series: correlations among sites were high, with an average of  $0.89 \pm 0.08$ ; and, southern New Brunswick had the lowest average wind chill while WNS had the highest. The temporal evolution of the CAO is clearer for wind chill than temperature with the onset at St. Stephen, and the largest lag of 6 h at Shearwater.

The February 2023 CAO was an extreme event: for four hours a wind chill of  $-37^{\circ}\text{C}$  was recorded at Shearwater RCS (solid red line, Fig 5); these were the lowest, hourly wind chills recorded at that location for all Februarys from 1994 through 2023. From Feb. 3, 21:00 to Feb. 4, 14:00 wind chill fell into the lowest 1% of 1993 to 2023 February values (lower red-dashed line, Fig 5), and air temperatures (solid blue line, Fig 5) were in the lower 1% from Feb. 3, 23:00 to Feb. 4, 12:00 (lower blue-dashed line, Fig 5). Significant heat loss from the ocean to the atmosphere would be expected for these conditions.

### Model sea-surface temperature changes during the CAO

To identify areas of interest, we first analyse the broader-scale response of the ocean using model results. Fig 6 shows broad-scale maps of daily-averaged sea-surface temperature (SST) from CIOPS-E from before (Feb. 2) and after (Feb. 5) the CAO, and the difference between the two. The SST differences show that several bays and

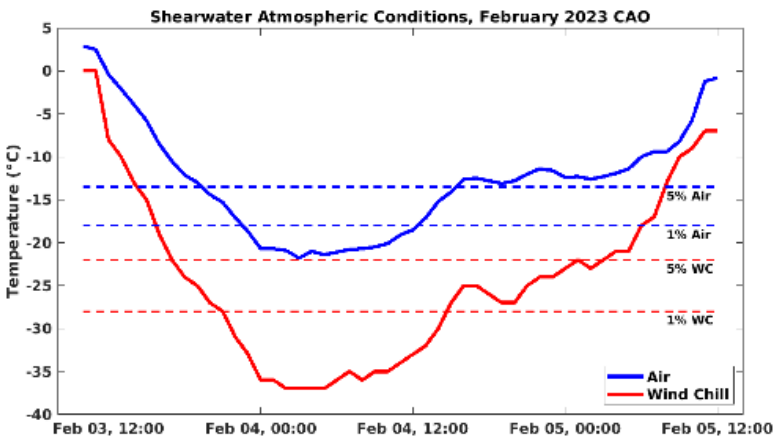


**Fig 5** Time series of air (blue solid) and wind chill (red solid) temperatures ( $^{\circ}\text{C}$ ) at Shearwater during the February 2023 CAO. The red and blue-dashed horizontal lines indicate the lower 1 and 5 percentile bins for all February hourly observations from 1994 to 2023 (12824 temperature observations, and 8627 measurable wind chills).

larger shallow areas of coastal Nova Scotia experienced significant cooling of up to 3°C over the course of the CAO. The locations are: St. Margaret's Bay and Mahone Bay on the South Shore; the south-western tip of Nova Scotia (Cape Sable and off Pubnico); St. Mary's Bay, and Chignecto and Cobequid Bays in the innermost reaches of the Bay of Fundy (see labels, top panel, Fig 7). Except for the South Shore locations, these sites are part of, or near to, the Gulf of Maine and Bay of Fundy which feature large tidal currents and consequently substantial mixing.

We choose mainly to focus our study on the aforementioned coastal locations of Nova Scotia. However, several other coastal areas within the CIOPS-E domain also experienced significant cooling indicating the broad spatial scale response to the CAO (bottom panel, Fig 6): a small area outside Passamaquoddy Bay, New Brunswick; the area off Bar Harbor, Maine, USA; and areas around Cape Cod, Massachusetts, USA. Other areas of large temperature changes on the Scotian Shelf and off the continental shelf are associated with eddies and current meanders; these may or may not have been influenced by the CAO. Analysis of such is beyond the scope of this study.

The southern coast along Anticosti Island in the Gulf of St. Lawrence experienced a substantial *increase* (by ~3°C) in SST during the CAO. This warming is consistent with the upwelling of warmer subsurface water, which would have to come from ~125 m depth based on long-term temperature and salinity climatology (Petrie *et al.* 1996). Based on the Ekman flux, we estimate that the WNW winds that were blowing parallel to the coast of Anticosti Island for most of the CAO (Fig 3) could have made a significant contribution to the upwelling of as much as ~40 m.

Less obvious cooling also appears in narrow near-shore bands along the Atlantic coast of Nova Scotia. The complicated coastlines of this area are not well resolved by the model which may lead to differences with observations.

Modelled SST and sea-bottom temperatures (SBT) at the nearshore study locations (Fig 7) that experienced rapid cooling were not substantially different (not shown). This, combined with the bathymetry of the area (Fig 1), indicates which regions are most susceptible to rapid cooling, namely shallow areas that are easily vertically mixed because of weak stratification and/or strong tidal flows, and do not have ready access to warmer/deeper waters to replenish the local

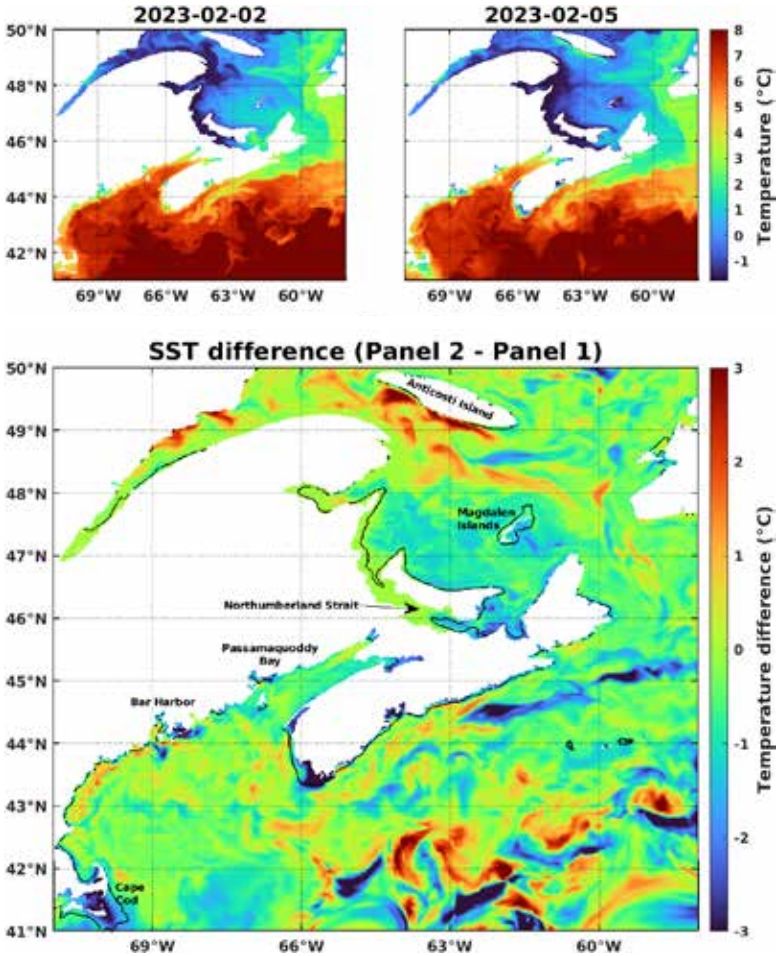


Fig 6 Model daily-average sea-surface temperatures ( $^{\circ}\text{C}$ ) for (top left) Feb. 2, and (top right) Feb. 5, 2023, and (bottom) the difference (Feb. 5-Feb. 2) between the two maps. The thin, black line in the lower panel is the 20 m bathymetric contour.

surface heat loss. During this outbreak, areas that experienced cooling are generally those with very shallow depths ( $< 20$  m, see 20 m bathymetric contour, bottom panel, Fig 6), with temperatures several degrees above freezing before the event onset. In deeper areas, the warmer waters present at depth can be a source of heat that reduces the near-surface temperature drops through vertical mixing or advection.

### **Temporal evolution of SST in select bays and nearshore areas**

To better quantify the response to the CAO in the affected bays, hourly SST time series (middle panel, Fig 7) were extracted from the model at the indicated locations (upper panel, Fig 7). Sudden drops of SSTs during the CAO (shaded in light grey in the middle panel) are important at all locations, on the order of 3°C, with little to no comparative cooling for several days leading up to the CAO. To varying degrees, all locations exhibit temperature fluctuations caused by the semi-diurnal tides moving horizontal temperature gradients at each site. To quantify the temperature drops, the tides were filtered out using a fourth-order low-pass 24-hr Butterworth filter (lower left panel, Fig 7). From the combined filtered and unfiltered results, two temperature behaviours are of note.

Mahone Bay (dark blue) and St. Margaret's Bay (orange) experienced rapid cooling, with temperatures dropping from approximately +1.3 to -1.7°C in both bays, reaching freezing temperatures for salt water midway through the CAO. Temperature variations from the tidal cycle, which were small at the beginning, are much reduced or gone, indicating that horizontal SST gradients have largely been eliminated in these somewhat isolated, shallow areas.

The other locations, which are in areas of strong tidal flows, exhibit temperature fluctuations of varying amplitude associated with the tidal cycle which persist during and after the CAO; this indicates that horizontal temperature gradients have not been eliminated by the surface cooling. Cape Sable (light blue) shows the largest temperature drop, ~6.5°C, from +5.8 to -0.6°C. The smallest drop of 2°C occurred in Chignecto Bay (black), from +1.5 to -0.5°C. The lower right panel of Fig 7 summarizes the modelled responses for each site.

### **Water temperature variations along St. Mary's Bay**

Location within an individual bay can be important. For example, SST in the inner and outer areas of St. Mary's Bay (iSMB and oSMB, purple and yellow curves in Fig 7) show significant differences. The oSMB site is warmer by ~2°C, and in an area where there are substantial horizontal temperature gradients and large tidal excursions (Petrie *et al.* 1996, DFO 2022) hence the temperature varies by up to 6°C with the tides. At iSMB, both the horizontal SST gradient and the tidal excursions are smaller, hence the tidal variation of temperature is also much smaller, 0.25°C. At both iSMB and oSMB

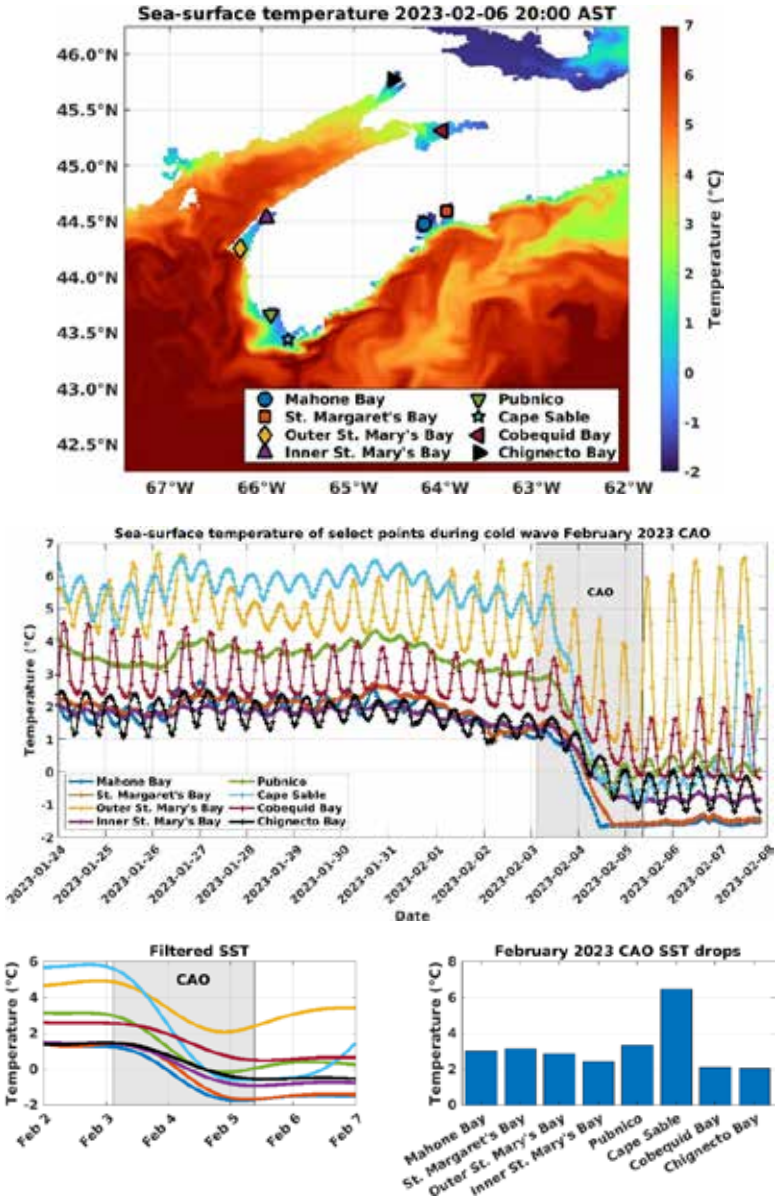


Fig 7 Top: Model SST (°C) on Feb. 6, 2023, 20:00 AST (after the CAO), and the selected locations for evaluation. Middle: hourly SST time series of model results at those locations before, during, and after the CAO (shaded grey); the colours of the curves match the colour of the symbols in the map. Bottom left: SST, filtered to remove the tidal signal centred on the CAO. Bottom right: calculated SST drops during the CAO from the filtered data.



the cooling associated with the CAO is overlaid on the tidal signal, with temperatures drops of 2.5 and 3.0°C, respectively.

To illustrate the differences along the length of St. Mary's Bay, a transect along the middle of the bay has been sampled from the model (see map, blue-dashed line, top panel of Fig 8). Hovmöller diagrams of this transect are shown in the lower three panels of the same figure (time on the x-axis, latitude on the y-axis), indicating the evolution of SST, SBT, and the difference between the two (SBT-SST). The evolution of the temperature is clear: before the CAO there is a substantial temperature gradient along the transect that moves with the tides, the waters then cool during the CAO. The difference (SBT-SST) in temperature is ~0°C throughout the period shown, indicating that the transect is vertically well mixed. The only substantial differences between SBT and SST are at the southern-most parts of the transect, south of ~44.15°N, in deeper waters beyond the entrance of SMB, and only appear near the end of the CAO. After the CAO, SST and SBT in the outer areas begin to recover as heat is replenished from the deeper adjacent regions; however, the inner bay remains cold, enhancing the original temperature gradient along SMB.

### **Comparison of modelled and observed water temperatures during the CAO**

Water temperature observations were obtained from eight moorings (locations, Fig 2), all showing significant cooling during the CAO (blue lines, Fig 9). The observed water temperature changes during the CAO, defined by the filtered series and black lines over blue lines, Fig 9, range from 1.0 (Halifax) to 3.9°C (Yarmouth), with an overall average cooling of ~3.0°C (Table 1). This range is comparable to that from the model at its closest location to each observation site (red lines), Fig 9, with filtered series overlaid in black ranging from 1.1 (Port Hawkesbury) to 3.5°C (Shelburne) (Table 1), with an average cooling of 2.3°C. At 5 of the 8 sites, observed temperatures before the onset of the CAO were greater than the modelled values by as much as ~2.5°C (Lunenburg).

The observed and modelled temperature changes at each individual site show evident differences, in particular at Canso where the observed cooling exceeded the model's result by 2.4°C. On the other hand, at Halifax the cooling estimated by the model was 1.5°C greater than observed. Some differences can be attributed to the fact that the model does not properly resolve the coastline features of the



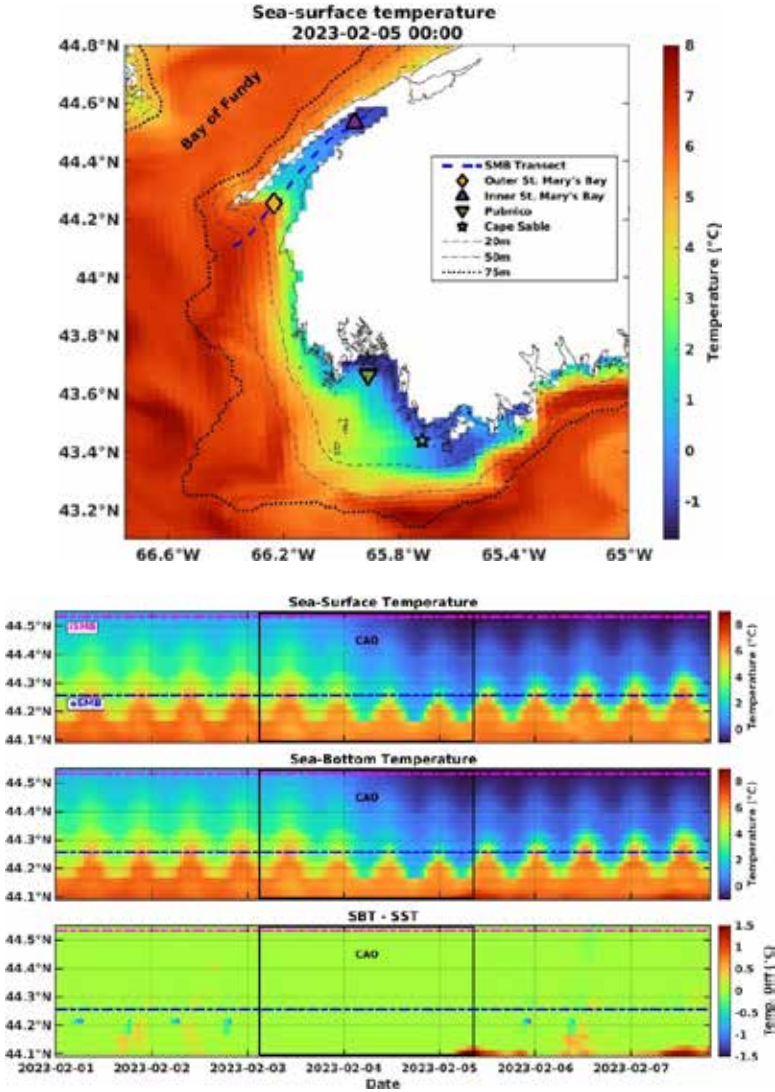


**Fig 8** Top: Model SST (°C) on Feb. 5, 2023, 00:00 (near the end of the CAO) off southwest Nova Scotia, local bathymetry (black dashed lines at indicated depths), and St. Mary's Bay (SMB) transect (blue-dashed line). 2nd, 3rd and 4th panels: Space-time variations of SST, SBT, and the difference between the two (SBT-SST), respectively, along the SMB transect. The locations of iSMB (magenta lines) and oSMB (blue lines) are indicated in each of the bottom three panels. In the lower panels, the latitudes indicate the location along the SMB transect, and hence how these quantities vary over time at each position. The vertical black lines mark the beginning and end of the CAO.

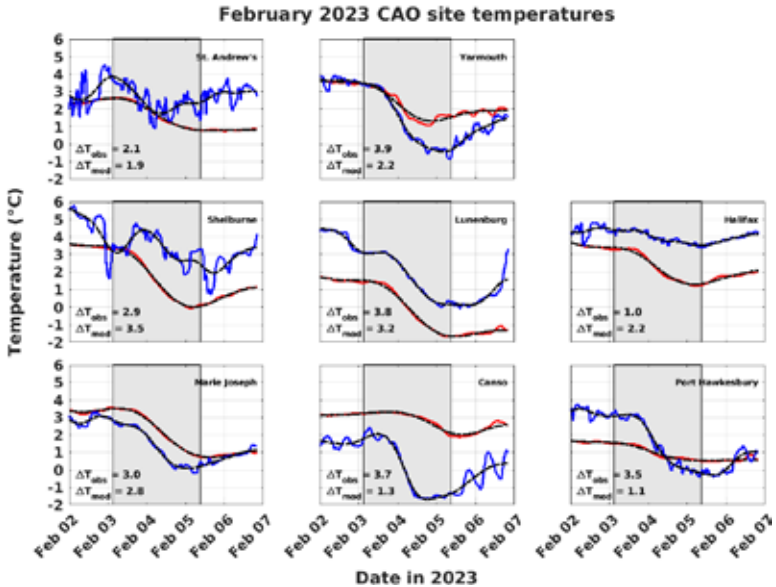


**Fig 9** Water temperatures ( $^{\circ}\text{C}$ ) from the model (red) and moorings (blue) during the February 2023 CAO (shaded areas) at the indicated locations in Fig 2, along with filtered responses (black lines) used to determine the temperatures changes at each location.

nearshore mooring sites, e.g. Halifax inlet is not captured. Moreover, the largest difference between modelled and observed cooling is at Canso where the mooring site is in a shallow and sheltered harbour, whereas the closest model grid point has a much larger depth of 82 m. The smaller temperature change in the model may be attributed the greater depth to spread the heat loss to the atmosphere, and the potential for a compensating heat flux from deeper depths through vertical mixing and/or advection.

### Sea ice in the Northumberland Strait and other areas

The Northumberland Strait between Prince Edward Island and Nova Scotia/New Brunswick is a shallow area susceptible to rapid cooling during a CAO. However, the SST differences from Fig 6 (lower panel) show no rapid cooling there during the February 2023 CAO. Prior to the CAO on Feb. 2 (left panel), the minimum SST ( $\sim -1.7^{\circ}\text{C}$ ) had already been reached, hence further heat loss will cause ice formation and thickening. Maps of the ice thickness ( $> 0.01\text{ m}$ ) from CIOPS-E show this to be the case (Fig 10). Before the CAO, ice covers the western half of the Northumberland Strait (upper left

panel). Afterwards, ice thickened in many areas, and formed in the eastern areas of the Strait that were previously ice free (upper left and bottom panels). Ice formation is evident in the western Gulf of St. Lawrence and around the Magdalen Islands. Some ice thickening and formation may be due to the wind and water currents moving the ice around, which could compact ice along the coast, or open leads for new ice to form.

During the CAO, the CIOPS-E ice cover in the Northumberland Strait compares favourably to the sea ice concentration estimates available from the Canadian Centre for Meteorological and Environ-

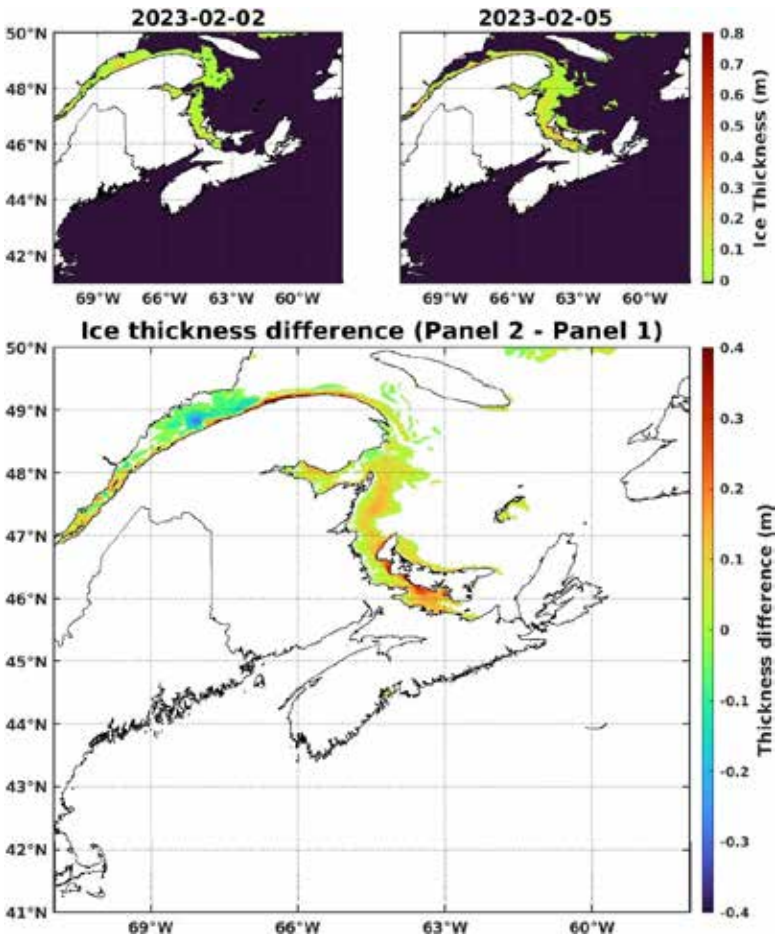


Fig 10 Model ice thickness (m, top left) before and (top right) after the CAO, and (bottom) the difference between the two.

mental Prediction (CCMEP) SST analysis (Fig 11, see Brasnett 2008; Brasnett and Surcel-Colan 2016, for descriptions of the data products). Both CIOPS-E and the CCMEP ice concentration estimates show the ice cover progressing eastward along the Northumberland Strait during the CAO, with CCMEP indicating more ice along the northern shore of Prince Edward Island. Of further note, CIOPS-E suggests ice formation in Mahone and St. Margaret's Bays during the CAO (Fig 10). The SST time series predicted by the model for these locations (Fig 7) suggest how ice formation would progress: prior to the CAO, SST was between 1.0 and 1.5°C, which then rapidly dropped to freezing temperatures ( $\sim -1.6^\circ\text{C}$ ) at around midday on Feb. 4, at which point ice formation would begin. However, there were no reports of ice in either bay. Moreover, during the CAO, observed near-surface water temperatures at Lunenburg (on the western edge of Mahone Bay) were about 1.5°C warmer than the model estimates (Fig 9), and remain well above ice formation temperature. This suggests that ice formation in the two bays was unlikely during the CAO. The difference between the model prediction and the observations appears related to the initial conditions (model temperature was  $\sim 2.5^\circ\text{C}$  colder) before the onset of the CAO. The cooling predicted by the model and that observed were similar (3.2°C versus 3.8°C). In contrast, observations at Canso approached freezing temperatures, suggesting that ice might begin to form if the CAO had persisted; on the other hand, model predictions were  $\sim 3.5^\circ\text{C}$  warmer (Fig 9).

## DECEMBER 2016 COLD AIR OUTBREAK

From December 15 to 18, 2016, Atlantic Canada experienced a CAO that was very similar to the one in February 2023 (compare Fig 3 and 12). Fig 13 shows air temperatures and wind chills (upper panel), and wind speeds (middle panel) at the same weather stations as for the February 2023 event. Wind speeds (solid lines) and 'to' directions (red flags, both bottom panel) are shown for a representative subset of those stations at times focused on the CAO. The CAO began part way through Dec. 15, and ended in the early hours of Dec. 17 (shaded areas), lasting slightly less than two days. The coldest average temperatures ( $\sim -17^\circ\text{C}$ ) during the CAO were recorded in southern New Brunswick, the warmest ( $\sim -9^\circ\text{C}$ ) in SWNS. Lagged correlations indicate no significant difference in the timing of the

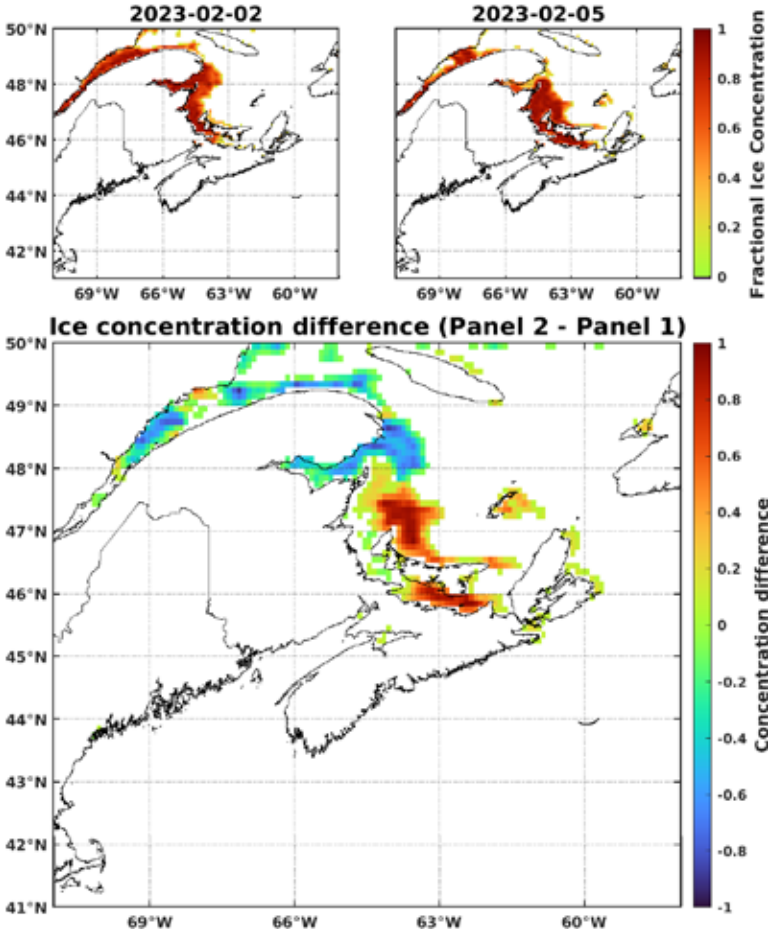
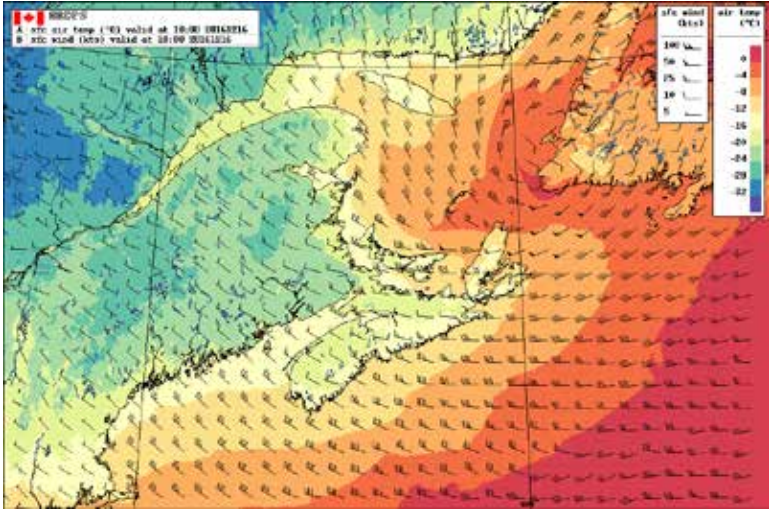


Fig 11 Satellite estimates of ice concentration before and after the February CAO (upper panels; color shading for fractional ice coverage  $> 0.15$ ). Lower panel: Difference (Feb. 5-Feb. 2) between ice coverage  $> 0.10$ .

event across the region. The average correlation between the air temperature series was 0.81 with a standard deviation of 0.14, less coherent than in 2023. Strong, predominantly WNW winds, like the February 2023 CAO, prevailed over the region. The strongest winds were seen at Brier Island and Baccaro Point, with peak speeds of  $\sim 80$  km/h at the former. The variation of wind chill during the CAO was very similar to the air temperature series: correlations among sites were high, with an average of  $0.86 \pm 0.10$ . The region experienced





**Fig 12** HRDPS-predicted 1.5 m air temperatures and 10 m winds on Dec. 16, 2016, 06:00 AST (10:00 UTC).

wind chills as low as  $-37^{\circ}\text{C}$ . Air temperatures and wind chills were extreme compared to hourly December weather conditions for Shearwater from 1993-2022 (Fig 14). Air temperatures were in the lowest 1% of values ( $< -13^{\circ}\text{C}$ ) for approximately 30 hours beginning on Dec. 16, 02:00. Wind chills were in the lower 1% and 5% of values for 12 and 31 hours, respectively. Significant heat fluxes from the ocean to the atmosphere would have occurred.

### Large-scale response of the model

Compared with the February 2023 CAO, the December 2016 CAO occurred  $\sim 50$  days earlier in the fall/winter season when higher, but gradually decreasing, SSTs would be expected. This is confirmed by CIOPS-E time-series of SSTs (upper panel, Fig 15, same locations as in Fig 7) that show gradual cooling in the weeks prior to and rapid cooling during the CAO (shaded area). Daily average SST maps before (Dec. 15) and after (Dec. 17) the CAO, as well as the difference between the two dates, show cooling patterns similar to the February 2023 CAO in the various bays of interest (Fig 16). There was cooling in the Northumberland Strait, as ice was not present in the region (not shown), with warm enough initial SSTs for the CAO to have an affect here as well. As in 2023, Cape Sable had the largest temperature drop (bottom panels, Fig 15),  $6.3^{\circ}\text{C}$ , from approximately  $7.6$  to  $1.3^{\circ}\text{C}$ ;

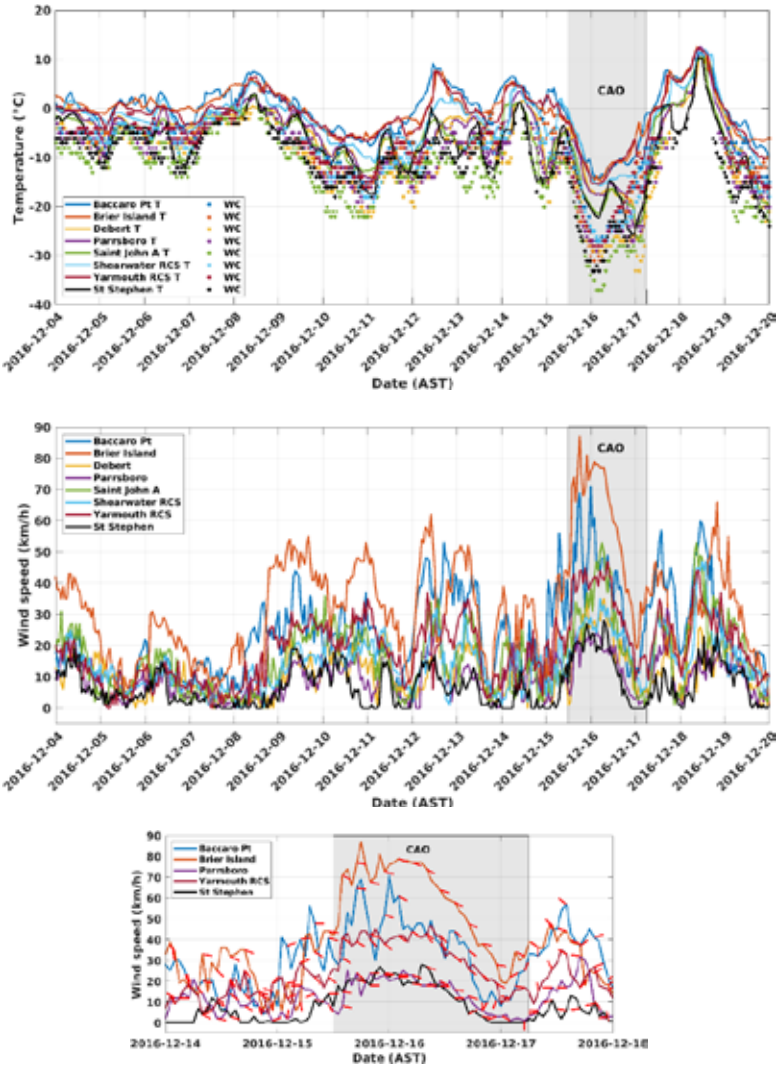


Fig 13 Top panel: air temperatures (T; solid lines, °C) and wind chills (WC; '+' signs, °C) as measured by the ECCC stations in Fig 1. Middle panel: wind speeds (km/h) at the same sites. Lower panel: wind speed (solid lines) and 'to' directions (short red lines).

it then rebounded a couple of days later from the intrusion of warmer water. The minimum temperature drop was in Cobequid Bay, 1.7°C, from 5.8 to 4.1°C. All other locations experienced decreases of 1.8 to 2.9°C, including sites in SMB of 2.1°C.



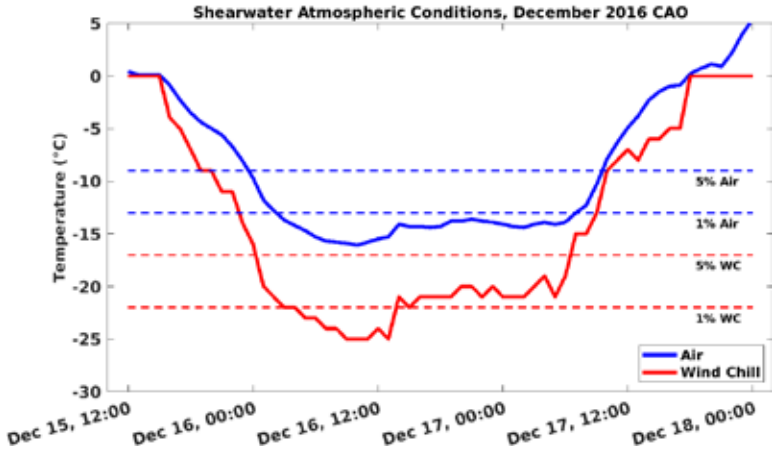


Fig 14 Time series of air (blue solid) and wind chill (red solid) temperatures (°C) at Shearwater during the December 2016 CAO. The red and blue-dashed horizontal lines indicate the lower 1 and 5 percentile bins for all December hourly observations from 1993 to 2022 (21810 temperature observations, and 9043 measurable wind chills).

### Observations at select sites

Temperature observations ( $T_{\text{obs}}$ ) were available from 15 coastal sites (Fig 2) to compare with the model ( $T_{\text{mod}}$ ). Filtered  $T_{\text{obs}}$  (Fig 17, Table 1) indicate temperature decreases of 1.0°C (mouth of Mahone Bay) to 3.7°C (Canso); temperature drops in the model were from 0.4°C (Sandford) to 6.3°C (Cape Sable). The averages of the temperature changes associated with the CAO were 1.9°C for the observations and 2.2°C for the model. However, 10 records had the observed temperatures up to ~4°C greater than model values; at 4 sites, the observed and modelled temperatures were essentially equal. As for the 2023 CAO, at Canso the observed temperatures were substantially lower (by 2-5°C) than the model predictions.

From outer St Mary's Bay (Grand Passage, Saulnierville, Meteghan) to the mouth of Mahone Bay, the general tendency is for  $\Delta T_{\text{obs}} < \Delta T_{\text{mod}}$ , with an average value of 1.2°C, where  $\Delta$  indicates a temperature change. Within this group the largest difference, 4.5°C, is for Cape Sable. From Halifax through Sydney the opposite is observed,  $\Delta T_{\text{obs}} > \Delta T_{\text{mod}}$ , on average by 0.9°C. The largest difference is for Canso.

Animations of model SST of the area (not shown), and consideration of the wind direction (WNW) give clues to the model response for both CAOs at Cape Sable. Prior to each CAO, Cape Sable is

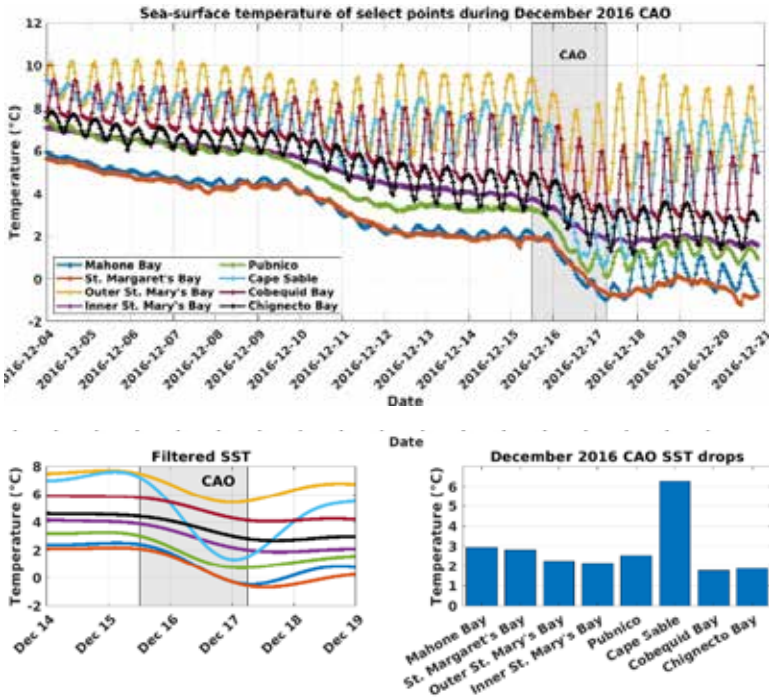


Fig 15 Top: hourly SST time series (°C) of model results at selected locations (see Fig 7, upper panel) before, during, and after the CAO for the December 2016 CAO. Bottom left: SST filtered to remove tidal signals centred on the CAO. Bottom right: calculated SST drops during the CAO from the filtered data.

considerably warmer than Pubnico. The CAO wind then drives the colder water in the Pubnico region in the direction of Cape Sable. So, part of the cooling at Cape Sable is from advection of colder water into the area that dominates local cooling. After the CAO, wind patterns change, and warmer waters flow back to Cape Sable, restoring the initial conditions that prevailed in December 2016. Compared to observations, the model appears to be overestimating the temperature gradient between Pubnico and Cape Sable.

Observations in iSMB (where the latter stages of the fish kill occurred) are not available. The model predicts a drop of about 2°C in the area; however, given the lack of *in-situ* data for verification, this is not sufficient to conclude that the CAO contributed to the fish kill.

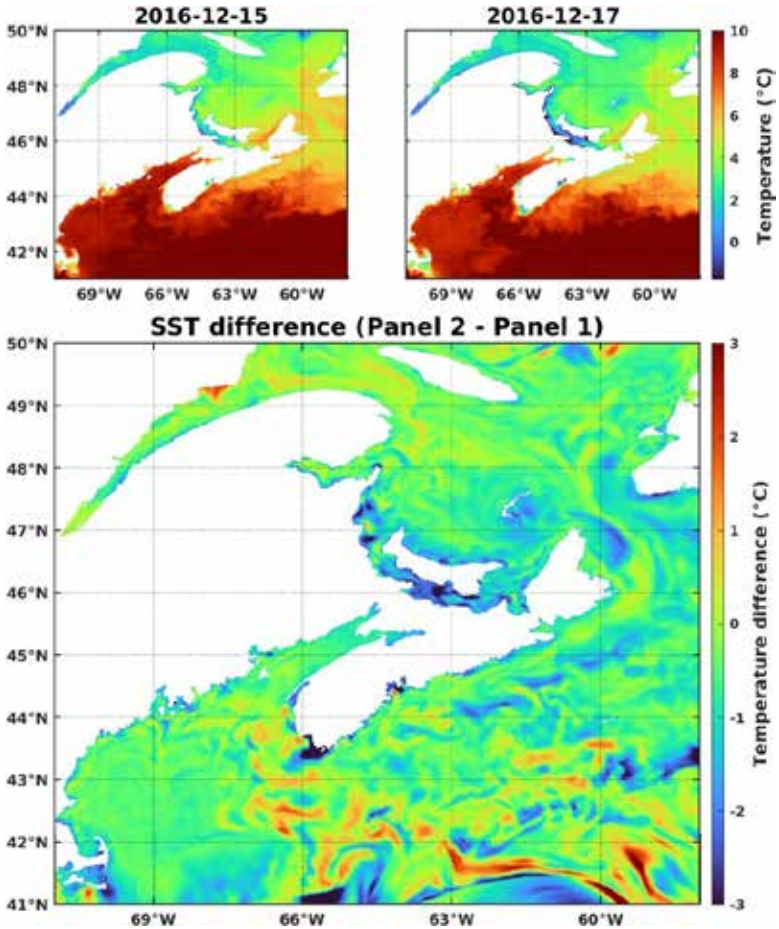


Fig 16 Model daily-average sea-surface temperatures ( $^{\circ}\text{C}$ ) for (top left) Dec. 15 and (top right) Dec. 17, 2016, and (bottom) the difference (Dec. 17-Dec. 15) between the two maps.

## CONCLUSIONS

The recently developed CIOPS-E system provides short-term (48h) operational forecasts and continuous “pseudo-analysis” of past (2016-present) ocean conditions in Atlantic Canada. Here, we analyzed the space-time variations of ocean temperature from the pseudo-analysis during two short-lived (2.5 days or less), extreme cold air outbreaks in December 2016 and February 2023 for coastal areas from Cape Breton to the Bay of Fundy. For both events, model

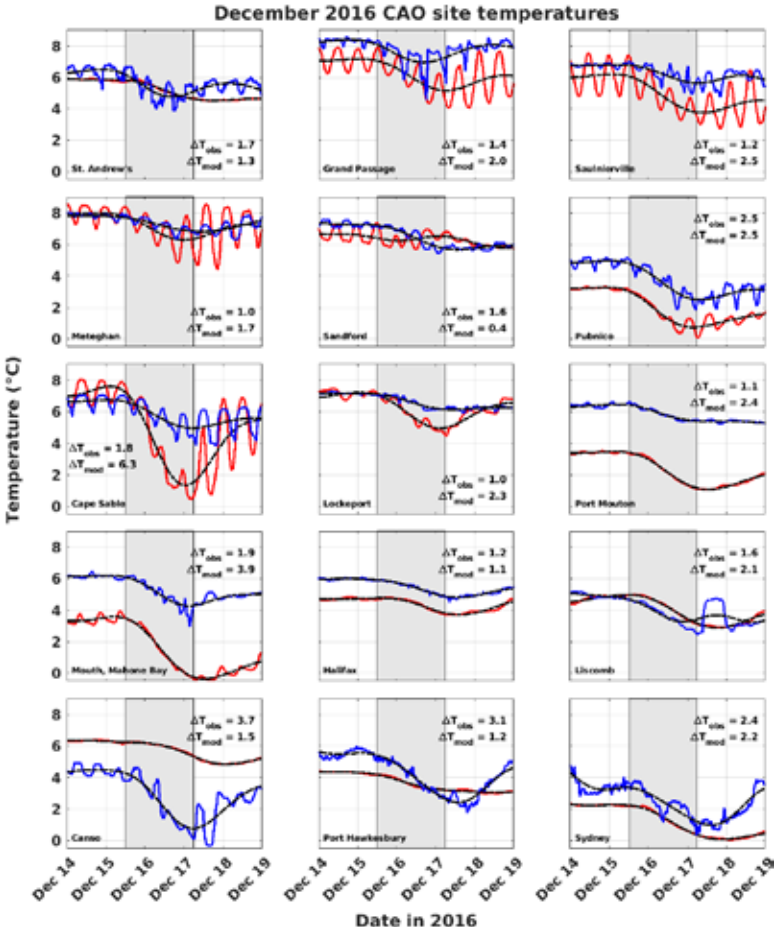


Fig 17 Water temperatures (°C) from the model (red) and moorings (blue) during the December 2016 CAO (shaded areas) at the indicated locations, along with filtered responses (black lines) used to determine the temperatures changes at each location.

results show SST drops of 1.5 to 5°C in relatively isolated shallow bays and straits. Regional averages of the temperature changes at common observation and model sites agreed to within 0.3°C (2016) and 0.7°C (2023), though differences between individual sites were large, -1.2°C to 2.4°C in 2016, and -4.5°C to 2.2°C in 2023. Overall, this suggests that the model is capturing the heat flux from the coastal ocean to the atmosphere during a CAO event. At the scale of individual bays, this is not the case. The mismatch of initial conditions

in the model as compared to the observations, and inadequate resolution of coastal topography, have been identified as two potential sources of these discrepancies. In addition, there are systematic differences between model estimates and observed temperatures, namely, for the 2016 CAO, model values were greater than observations for the western half of the region, less for the eastern half; for the 2023 event, model temperatures were greater for the eastern half. These results suggest that broader scale intercomparisons of temperature fields over the adjacent shelf are warranted. One could then determine if mixing with, and advection of, deeper, offshore waters are captured properly by the model.

Around Nova Scotia, the model identifies bays and regions that are particularly susceptible to rapid cooling: St. Margaret's, Mahone, St. Mary's, Cobequid, and Chignecto Bays, as well as the Pubnico/Cape Sable shallow areas immediately off the coast of southwest Nova Scotia. Shallow areas with reduced access to deeper waters, either through mixing or advection, should be more vulnerable to rapid, substantial cooling. The Northumberland Strait between Nova Scotia and Prince Edward Island can also experience rapid cooling and ice formation. The ice modelling reported for the 2023 CAO event successfully reproduced the observed ice formation and growth in the Strait and western Gulf of St. Lawrence, providing support for the validity of the model.

Fish kills have been attributed to CAOs in Florida and Japan. An extensive mackerel die-off in Newfoundland occurred during a sustained period of cold temperatures and low wind chills. The December 2016 CAO featured a sudden drop in water temperatures that might have contributed to the latter stages of the concurrent fish kill in St. Mary's Bay, although a definitive explanation has not been reached. Nonetheless, this study has shown that operational ocean forecasts have the potential to be useful tools that will benefit the siting, assessment, protection and management of marine ecosystems, fishing resources, and the aquaculture industry.

*Acknowledgements* We are grateful to ECCC for providing the atmospheric observational and ocean forecasting data, and the development of the CIOPS-E system. Many colleagues helped this study by providing advice and comments, particularly David Brickman, David Greenberg, Li Zhai, Rachel Horwitz, Stephanie Taylor, François Roy,

and Gregory Smith. We particularly appreciate the many inspiring discussions with the late Professor Keith Thompson of Dalhousie University regarding the December 2016 CAO event. We thank the reviewers for their insightful and constructive comments, and the journal Editors for valuable instructions.

We are grateful to the following sources for the *in-situ* data used in this study: the Fishermen and Scientists Research Society (fsrcs.ca, contact Shannon.Scott-Tibbetts@dfo-mpo.gc.ca); the Bedford Institute of Oceanography, DFO contacts: Claudio.DiBacco@dfo-mpo.gc.ca, funding from DFO-Maritimes Biofouling Monitoring Program; Adam.Drozowski@dfo-mpo.gc.ca, funding from Transport Canada, World Class Tanker Safety Systems; and Ed.Horne@dfo-mpo.gc.ca, DFO Long Term Temperature Monitoring Program), St. Andrews Biological Station, DFO (contact Jack.Fife@dfo-mpo.gc.ca).

We acknowledge funding support from Fisheries and Oceans Canada, through the Marine Conservation Target (MCT) Program.

## REFERENCES

- Brasnett, B.** (2008). The impact of satellite retrievals in a global sea-surface temperature analysis. *Quarterly Journal of the Royal Meteorological Society* 134: 1745-1760. doi:10.1002/qj.319.
- Brasnett, B. & Surcel-Colan, D.** (2016). Assimilating retrievals of sea surface temperature from VIIRS and AMSR2, *Journal of Atmospheric and Oceanic Technology* 33(2): 361-375. doi:10.1175/JTECH-D-15-0093.1.
- Department of Fisheries and Oceans Canada.** (2017). Stock status update of 4VWX herring. DFO Canadian Science Advisory Secretariat Response, 2017/137. waves-vagues.dfo-mpo.gc.ca/library-bibliotheque/40626337.pdf
- Department of Fisheries and Oceans Canada.** (2022). Canadian Atlas of Tidal Currents, Volume 1 : Bay of Fundy and Gulf of Maine 2015 / Canadian Hydrographic Service, Fisheries and Oceans Canada. cat.fsl-bsf.scitech.gc.ca/record=b4105151~S1
- Environment and Climate Change Canada.** (2023). Historical Climate Data, Environment and Climate Change Canada. Environment and Climate Change Canada. climate.weather.gc.ca/historical\_data/search\_historic\_data\_e.html on 2023-06-01
- Foley, M., Askin, N., Belanger, M. & Wittnich, C.** (2019). Body condition and heavy metal levels in 2016 Atlantic herring (*Clupea harengus*) fish kill stranding event in Nova Scotia, Canada. *Journal of Marine Animals and Their Ecology* 11(2): 18-28.



- Gasset, N.** (2019). Global Deterministic Prediction System (GDPS), update from version 6.1.0 to version 7.0.0. 2021. [collaboration.cmc.ec.gc.ca/cmc/cmoe/product\\_guide/docs/tech\\_specifications/tech\\_specifications\\_GDPS\\_e.pdf](https://collaboration.cmc.ec.gc.ca/cmc/cmoe/product_guide/docs/tech_specifications/tech_specifications_GDPS_e.pdf)
- Gilmore, R. G., Bullock, L. H. & Berry, F. H.** (1978). Hypothermal mortality in marine fishes of south-central Florida, January, 1977. *Gulf of Mexico Science* 2(2): 1. doi:10.18785/negs.0202.01.
- Gomez, R., Tabalanza, T., Toyama, K., Herwening, L. K., Azuma-Malsol, M., Fujiwara, N., Yin, X. & Nakamura, T.** (2024). Fish mortality following sudden cold snap in Okinawa-jima Island, Japan. *Ichthyological Research* 71(1): 200-204. doi:10.1007/s10228-023-00914-4.
- Hunke, E.C.** (2001). Viscous-plastic sea ice dynamics with the EVP model: linearization issues, *Journal of Computational Physics* 170: 18-38. doi:10.1006/jcph.2001.6710.
- Hunke, E.C. & Lipscomb, W.H.** (2008). CICE: The Los Alamos sea ice model. Documentation and software user's manual version 4.0 (Tech. Rep. LA-CC-06-012), Los Alamos, NM: Los Alamos National Laboratory.
- Lipscomb, W.H., Hunke, E.C., Maslowski, W. & Jakacki, J.** (2007). Ridging, strength, and stability in high-resolution sea ice models. *Journal of Geophysical Research* 112 (C03S91). doi:10.1029/2005JC003355.
- Marsh, R., Petrie, B., Weidman, C., Dickson, R., Loder, J., Hannah, C., Frank, K. & Drinkwater, K.** (1999). The 1882 tilefish kill - a cold event in shelf waters off the north-eastern United States? *Fisheries Oceanography* 8(1): 39-49. doi:10.1046/j.1365-2419.1999.00092.x.
- Milbrandt, J.A., Bélair, S., Faucher, M., Vallée, M., Carrera, M.L. & Glazer, A.** (2016). The pan-Canadian high resolution (2.5 km) deterministic prediction system. *Weather Forecast* 31(6): 1791-1816. doi:10.1175/WAF-D-16-0035.1.
- Madec, G., et al.** (2015). NEMO ocean engine, Note du Pole de modélisation. France. Ver 3.6 stable, ISSN No 1288-1619.
- Paquin, J.-P., Roy, F., Smith, G.C., MacDermid, S., Lei, J., Dupont, F., Lu, Y., Taylor, S., St-Onge-Drouin, S., Blanken, H., Dunphy, M. & Soontiens, N.** (2024). A new high-resolution Coastal Ice-Ocean Prediction System for the east coast of Canada. *Ocean Dynamics*, in revision.
- Paquin, J.-P., Roy, F., Smith, G.C., Dupont, F., MacDermid, S., Hata, Y., Huizy, O., Lei, J., Lu, Y., Taylor, S. & Blanken, H.** (2022). Coastal Ice Ocean Prediction System for the East Coast of Canada (CIOPS-E) – System description for version 1. Canadian Centre for Meteorological and Environmental Prediction Technical Note. April 20th 2022. [collaboration.cmc.ec.gc.ca/cmc/CMOE/product\\_guide/docs/tech\\_notes/technote\\_ciops-east-100\\_e.pdf](https://collaboration.cmc.ec.gc.ca/cmc/CMOE/product_guide/docs/tech_notes/technote_ciops-east-100_e.pdf)
- Paquin J.-P., Roy, F., Smith, G.C., Dupont, F., MacDermid, S., Hata, Y., Huizy, O., Lei, J., Martinez, Y., Blanken, H., Holden, J. & Soontiens, N.** (2021). Coastal Ice Ocean Prediction System for the East Coast of Canada (CIOPS-E) – Update from version 1.5.0 to 2.0.0. Canadian



Centre for Meteorological and Environmental Prediction Technical Note.  
December 1st 2021.

[collaboration.cmc.ec.gc.ca/cmc/CMOI/product\\_guide/docs/tech\\_notes/  
technote\\_ciops-east-200\\_e.pdf](https://collaboration.cmc.ec.gc.ca/cmc/CMOI/product_guide/docs/tech_notes/technote_ciops-east-200_e.pdf)

**Petrie, B., Drinkwater, K., Gregory, D., Pettipas, R. & Sandstrom, A.** (1996). Temperature and salinity atlas for the Scotian Shelf and the Gulf of Maine. Can. Tech. Rep. Hydrogr. Ocean Sci. 171: v + 398 pp.

**Smith, G.C., Liu, Y., Benkiran, M., Chikhar, K., Surcel-Colan, D., Gauthier, A.-A., Testut, C.E., Dupont, F., Lei, J., Roy, F. & Lemieux, J.F.** (2021). The Regional Ice Ocean Prediction System v2: a pan-Canadian ocean analysis system using an online tidal harmonic analysis. *Geoscientific Model Development* 14(3): 1445-1467.  
doi:10.5194/gmd-14-1445-2021.

**Smith, E.T. & Sheridan, S.C.** (2020). Where Do Cold Air Outbreaks Occur, and How Have They Changed Over Time? *Geophysical Research Letters* 47(13): e2020GL086983. doi:10.1029/2020GL086983.

#### **News releases**

Seaward Enterprises Association of Newfoundland and Labrador via  
[fisherynation.com/sea-nl-calls-on-ottawa-to-lift-mackerel-moratorium-at-least-match-u-s-quota-for-2023](https://fisherynation.com/sea-nl-calls-on-ottawa-to-lift-mackerel-moratorium-at-least-match-u-s-quota-for-2023)

Seaward Enterprises Association [fisherynation.com](https://fisherynation.com)